Indian Geotechnical Journal, 33 (4), 2003

Analysis of Eccentrically-Obliquely Loaded Ring Footings on Sand

Swami Saran*, N.M. Bhandari† and M.M.A Al-Smadi‡

Introduction

Ring foundations (circular in plan with an annuli) are usually provided for tall circular structures like smoke stacks, cement silos, water towers etc. For such structures, the ring foundations are preferred because of full utilization of soil capacity and less or no tension condition under the foundation. These foundations generally are subjected to vertical load due to the superstructure and the horizontal load due to wind pressure acting on the structure.

Ring foundations have not attracted much attention of research investigators. In the past, attempts to develop analytical solution for estimating settlements, under reactive pressures using elastic theory (Egorov, 1965; Brodocheva, 1968) and also finite element technique (Milovic, 1973; Bowles, 1975) have been made. However, these studies pertain to foundations under axial vertical loads only. Experimental studies under both axial and eccentric vertical loads have also been reported (Saha, 1978; Haroon, 1980; Chaturvedi, 1982; Kakroo, 1985). Dimensional analysis approach has generally been adopted to analyse the experimental results (Kakroo, 1985). Attempts to measure contact pressure distribution below the base of ring footings have also been made by conducting model tests on instrumented foundations (Kakroo, 1985). However, there is no study reported in the literature where

* Emeritus Fellow, Department of Civil Engineering, Indian Institute of Technology Roorkee, Roorkee - 247667, Uttaranchal, India. E-mail: rajommce@iitr.ernet.in

† Professor, Department of Civil Engineering, Indian Institute of Technology Roorkee, Roorkee - 247667, Uttaranchal, India.

‡ Ministry of Public Works & Housing, Laboratory & Research Directorate, P.O. Box 1220, Amman, Jordan.

studies on ring footings subjected to a combination of axi-symmetrical vertical and lateral loading have been carried out. This is the problem of great practical relevance because the tall structures for which such foundations are provided are subjected to large lateral load due to wind. Thus, in addition to the vertical load, the base of these foundations is subjected to large moment and horizontal load. In other words, the ring foundations are in general subjected to eccentric-inclined load.

Bearing capacity, settlement and tilt are required for proportioning ring foundations subjected to eccentric inclined loads. Bearing capacity may be obtained using the equation proposed by Al-Smadi (1998), which is given later in this paper. The current practice of obtaining settlement and tilt of such foundations is based on many assumptions and, therefore, is very approximate.

Constitutive laws of soils define the mechanical behavior of soils and are of prime importance for analyzing almost all applied non-linear problems of soil mechanics. The most popular mathematical model for describing a constitutive law is a two constant hyperbola suggested by Kondner et al. (1963). The two constants of this model can be obtained by performing triaxial test on the pertaining soil simulating field condition.

In this paper, a new method has been suggested to obtain the pressure-settlement and pressure-tilt characteristics of an actual ring footing on sand subjected to eccentric inclined load using non-linear constitutive law of soil. The stress-strain behavior of sands is dependent on confining pressure. This fact has been taken into account in developing the analysis.

The method proposed herein has already been used earlier for getting pressure-settlement and pressure-tilt characteristics of actual strip and square footings (Prakash et al., 1984; Agarwal, 1986). They have analyzed six cases namely (i) smooth flexible strip footing, (ii) smooth rigid strip footing, (iii) rough flexible strip footing, (iv) rough rigid strip footing, (v) smooth flexible square footing and (vi) smooth rigid square footing. They concluded that the effects of roughness and rigidity of footing are very small on the average pressure-settlement and average pressure-tilt curves. Advantage of these conclusions has been taken in developing the proposed analysis for ring footings.

In general, ring footings have rough base and partial rigidity depending on the ring thickness. However as the effect of roughness and rigidity on the pressure versus average settlement, and pressure versus tilt curves are very small, for simplification of analysis, firstly the method is developed for smooth-flexible ring footing. In the end, an empirical but logical procedure has been suggested to obtain the settlement and tilt characteristics of the

corresponding rigid footing subjected to eccentric inclined load. The results may be slightly on the safer side and therefore can be used for actual rigid rough base ring footings.

Analysis

The analysis has been developed for studying the behavior of a ring footings subjected to eccentric-inclined load (Fig.1). The analysis is based on the following assumptions:

1. The soil mass is a semi-infinite and isotropic medium.

2. The footing base is smooth and flexible.

3. The whole area of the footing has been divided into m × n small parts (Fig.2). Each part is assumed to carry a concentrated load acting at its centre for determining stresses in the soil mass. The concentrated load

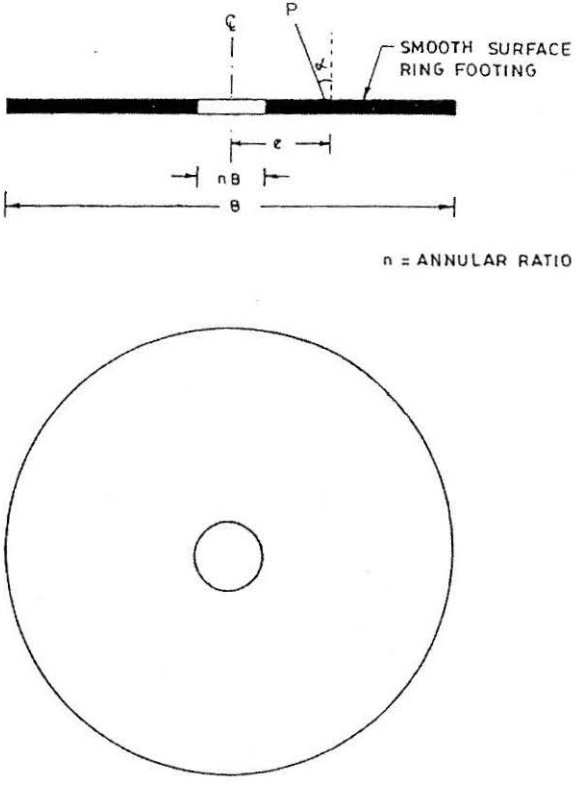

FIGURE 1 : Ring Footing Subjected to Eccentric Inclined Load

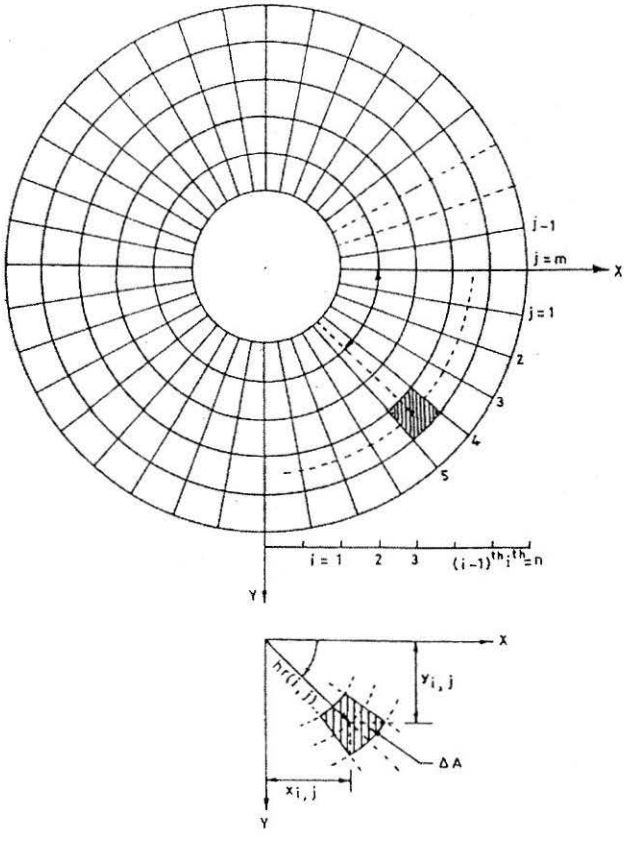

FIGURE 2 : Footing Area Divided into n Equal Rings and m Equal Sectors

is obtained by multiplying the average pressure intensity obtained from the contact pressure distribution shown in Figs.3 and 4 acting on the element by its area.

4. The eccentric-inclined load P acting on the footing is resolved into vertical and horizontal components (i.e. $P\cos\alpha$ and $P\sin\alpha$, Fig.1). The contact pressure distribution diagrams for both $P\cos\alpha$ and $P\sin\alpha$ components have been assumed linear (Figs.3 and 4). Following two cases have been considered, depending on the amount of the eccentricity:

Case 1

$$\frac{e}{B} \leq \frac{\left(1+n^2\right)}{8} \quad \text{(Fig.3)}$$

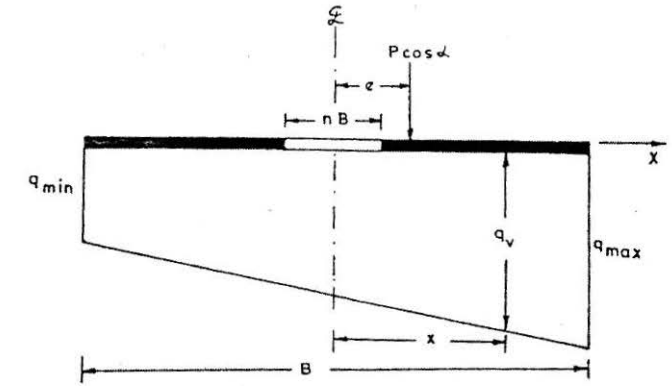

(a) CONTACT PRESSURE DIAGRAM DUE TO VERTICAL COMPONENT OF ECCENTRIC-INCLINED LOAD

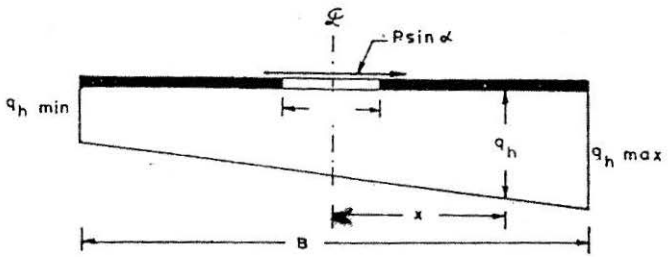

(b) CONTACT PRESSURE DIAGRAM DUE TO HORIZONTAL COMPONENT OF ECCENTRIC-INCLINED LOAD

FIGURE 3 : Assumed Contact Pressure Distributions for $e/B \leq \left[\left(1+n^2\right)/8\right]$

The contact pressure due to load components $P\cos\alpha$ (Fig.3a) and $P\sin\alpha$ (Fig.3b) at distance x from the centre are given by (Roark, 1954; Young, 1989):

$$q_v = \frac{P}{A}\cos\alpha\left[1+\left(\frac{8}{1+n^2}\right)\left(\frac{e}{B}\right)\left(\frac{x}{R}\right)\right] \tag{1}$$

$$\Delta P_v = q_v \cdot \Delta A \tag{2}$$

$$q_h = \frac{P}{A}\sin\alpha\left[1+\left(\frac{8}{1+n^2}\right)\left(\frac{e}{B}\right)\left(\frac{x}{R}\right)\right] \tag{3}$$

$$\Delta P_h = q_h \cdot \Delta A \tag{4}$$

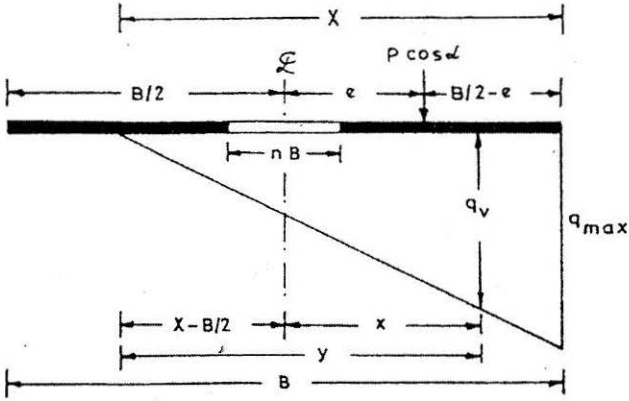

(a) CONTACT PRESSURE DIAGRAM DUE TO VERTICAL COMPONENT OF ECCENTRIC-INCLINED LOAD

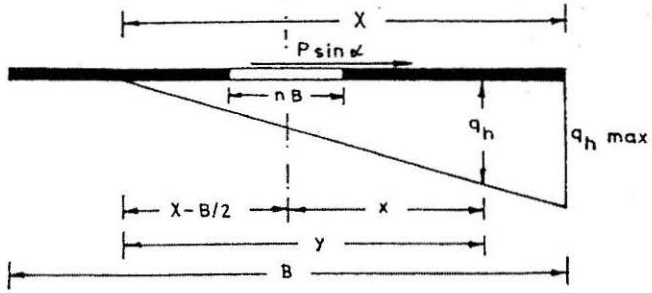

(b) CONTACT PRESSURE DIAGRAM DUE TO HORIZONTAL COMPONENT OF ECCENTRIC-INCLINED LOAD

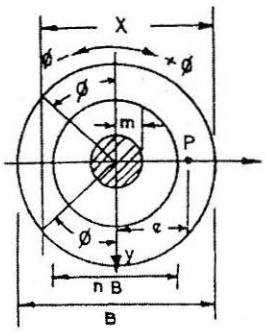

(c)

FIGURE 4 : Assumed Contact Pressure Distributions for $e/B > \left[\left(1+n^2\right)/8\right]$

where

P = Applied eccentric-inclined load

E = Eccentricity of the load

B = Diameter of the footing (= 2R)

α = Inclination of the applied load

A = Net area of the footing

n = Annular ratio

q_v = Contact pressure due to load component $P\cos\alpha$ at a point x

x = Coordinate of the point at which the contact pressure is desired

ΔA = Area of elementary strip

ΔP_v = Vertical point load acting in ΔA

q_h = Contact pressure due to load component $P\sin\alpha$ at a point x

ΔP_h = Horizontal point load acting in ΔA

Case 2

$$\frac{e}{B} > \frac{\left(1+n^2\right)}{8} \quad \text{(Fig.4)}$$

The maximum pressure due the vertical component of the eccentric-inclined load (Roark, 1954; Teng, 1977; Young, 1989) is given by:

$$q_{max} = k\left(P/A\right)\cos\alpha \tag{5}$$

As shown in Fig.(4a), the contact pressure, due to the vertical component of the eccentric-inclined load, at a point x from the centre of the footing is given by:

$$q_v = \left(y/X\right)q_{max} \tag{6}$$

$$\Delta P_v = q_v \Delta A \tag{7}$$

$$X = R\left(1-\sin\phi\right) \tag{8}$$

where X and ϕ are as shown in Fig.4(ii)c and ϕ satisfies Eqn.9.

$$\frac{e}{B} = \frac{(\pi/8) - 2.5\phi - (5/12)\sin\phi\cos\phi + (1/6)\sin^3\phi\cos\phi}{\cos\phi - (1/3)\cos^3\phi - (\pi/2)\sin\phi + \phi\sin\phi} \quad (9)$$

$$y = x + [X - (B/2)] \quad (10)$$

However, values of k and X/R have been calculated by Young (1989) for different n and e/R, and presented in Table 1.

The maximum contact pressure, due to the horizontal component of the applied eccentric-inclined load, as seen in Fig.(4b) taken as:

$$q_{h\,max} = k(P/A)\sin\alpha \quad (11)$$

The contact pressure due to the horizontal component at a point x is:

$$q_h = (y/X)q_{h\,max} \quad (12)$$

The soil mass supporting the footing is divided into a large number of thin horizontal strips (Fig.5).

There is no slippage at the interface of layers of the soil mass.

The stresses in each layer are computed using theory of elasticity. The strains are computed for the known stress condition using constitutive law.

Concept of Factor of Safety and Prerequisite of Approach

In sands, elastic modulus (E) and Poisson's ratio (μ) are dependent on confining pressure. Stress equations for such material are not available. Therefore, stress equations based on theory of elasticity (Boussinesq, 1885; Cerruti, 1888) have been used, and this fact has been taken into account by introducing a concept of factor of safety in the analysis. It will be seen later that this approach makes the predicted results very close to the real ones. This is illustrated in the next section.

The pre-requisite of the approach is to know the value of ultimate bearing capacity of a ring footing subjected to eccentric inclined load and resting on sand. For this, the following equation (Al-Smadi, 1998) may be used:

$$q_{uie} = \gamma(B/2)D_R \tan\phi\left[238 + 465n - 1420n^2 + 754n^3\right]\cdot R_{er}\cdot R_{ir} \quad (13)$$

Table 1 : Values of K and X/R for Contact Pressure and Width Calculation for Different Values of n and e/R

N		e/R															
		0.25	0.29	0.3	0.34	0.35	0.4	0.41	0.45	0.5	0.55	0.6	0.65	0.7	0.75	0.8	0.85
0.0	X/R	2.00	1.82			1.66	1.51		1.37	1.23	1.10	0.97	0.84	0.72	0.60	0.47	0.35
	k	2.00	2.21			2.46	2.75		3.11	3.56	4.14	4.9	5.94	7.43	9.69	13.4	20.5
0.4	X/R		2.00	1.97		1.81	1.67		1.53	1.38	1.22	1.05	0.88	0.73	0.60	0.48	0.35
	k		2.00	2.03		2.22	2.43		2.68	2.99	3.42	4.03	4.9	6.19	8.14	11.3	17.3
0.6	X/R				2.00	1.97	1.84		1.71	1.56	1.39	1.21	1.02	0.82	0.64	0.48	0.35
	k				2.00	2.03	2.18		2.36	2.58	2.86	3.24	3.79	4.64	6.04	8.54	13.2
0.8	X/R							2.00	1.91	1.78	1.62	1.45	1.26	1.05	0.84	0.63	0.41
	k							2.00	2.10	2.24	2.42	2.65	2.94	3.34	3.95	4.98	7.16

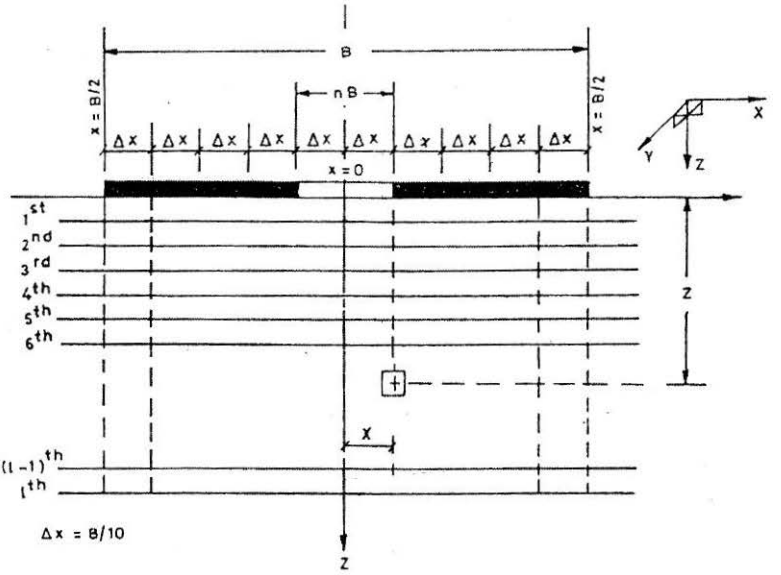

FIGURE 5 : Soil Mass Supporting a Footing Divided Equally into 1 Horizontal Layers

where q_{uie} = Ultimate bearing capacity of a ring footing subjected to eccentric-inclined load

B = External diameter of the ring footing (Fig.1)

γ = Unit weight of sand

D_R = Relative density of sand

ϕ = Angle of internal friction of sand at relative density, D_R

$$R_{er} = \left[1-(2e/B)\right]^2 \quad (14)$$

$$R_{ir} = \left[1-(\alpha/\phi)\right]^2 \quad (15)$$

e = Eccentricity (Fig.1)

α = Angle of load inclination (Fig.1)

The Eqn.(13) has been validated by large number of model tests (Kakroo, 1985; Al-Smadi, 1998). For ring footings subjected to central vertical load, the factors R_{er} and R_{ir} will be equal to unity.

General Procedure

1. For a given load, P on the ring footing, the contact pressure distribution at the interface of the footing base and supporting soil is taken as

shown in Figs.3 and 4, depending on the amount of eccentricity The contact pressure distribution is the loading pattern for the soil at the surface below the footing, and the stresses in the soil mass is induced according to this loading pattern.

2. The soil mass supporting the footing is divided into n layers as shown in Fig.5.

3. Taking any vertical section, the normal and shear stresses (σ_x, σ_y, σ_z, τ_{xy}, τ_{yz}, τ_{zx}) at the center of a layer at depth z below the footing are computed using the theory of elasticity (Poulos and Davis, 1973). The effect of the soil weight has also been taken into account for determination of the

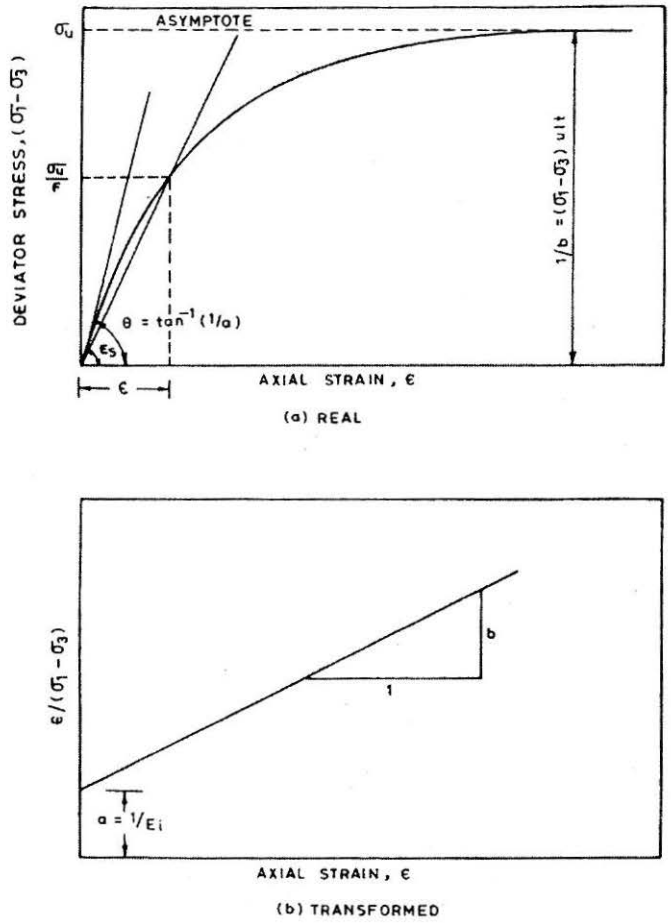

FIGURE 6 : Hyperbolic Representation of Stress-Strain (After Kondner, 1963)

total stresses in the soil mass. The vertical stress component due to weight of the soil has been taken as γz, where γ is the unit weight of the soil and z is the depth of the centre of soil layer. Whereas, the horizontal stress components (in x and y directions) have been taken equal to $K_o \gamma z$, where K_o is the coefficient of earth pressure at rest ($K_o = 1 - \sin\phi$), ϕ being the angle of internal friction. Thus the normal stresses considered are $(\sigma_x + K_o \gamma z)$, $(\sigma_y + K_o \gamma z)$ and $(\sigma_z + \gamma z)$.

4. The principal stresses $(\sigma_1, \sigma_2, \sigma_3)$ at a point in the soil mass and their directions $(\theta_1, \theta_2, \theta_3)$ with respect to the vertical z-axis are also computed using the theory of elasticity (Poulos and Davis, 1973).

5. The ultimate bearing capacity, q_{uie} is computed using Eqn.(13).

6. The factor 'F' for the given surface load intensity q has been obtained from the following relation :

$$F = q_{uie}/q \tag{14}$$

7. The constitutive equation for the supporting soil is obtained from triaxial compression test results using Kondner's two-constant hyperbola (Fig.6). It gives the relation as below:

$$\varepsilon_1 = \frac{a(\sigma_1 - \sigma_3)}{1 - b(\sigma_1 - \sigma_3)} \tag{15}$$

where ε_1 = Strain in the direction of principal stress σ_1 at deviator stress $(\sigma_1 - \sigma_3)$

σ_1, σ_3 = Major and minor principal stresses

a, b = Kondner's hyperbola constants (Fig.6b)

The modulus of elasticity E_s of the soil (Fig.6b) at any stress $(\sigma_1 - \sigma_3)$ is taken as:

$$E_s = \frac{(\sigma_1 - \sigma_3)}{\varepsilon_1} \tag{16}$$

The Eqns.(15) and (16) may be combined as

$$E_s = \frac{1 - b(\sigma_1 - \sigma_3)}{a} \tag{17}$$

In this approach, for a pressure intensity q, the value of E_s is taken corresponding to deviator stress σ_u/F, where F is the factor of safety computed in step 6. It means that:

$$E_s = \frac{1-b(\sigma_u/F)}{a} \tag{18}$$

The values of a and b may be obtained by plotting the triaxial test data as shown in Fig.6b. Both a and b are dependent on confining pressure

8. Evaluation of Strains: The strain ε_1 in the direction of major principal stress, σ_1, is determined as below:

$$\varepsilon_1 = \frac{(\sigma_1-\sigma_3)}{E_s} \tag{19}$$

The strains ε_2 and ε_3 are computed from the following relationships, which are based on theory of elasticity:

$$\varepsilon_2 = \frac{\sigma_2-\mu(\sigma_1+\sigma_3)}{\sigma_1-\mu(\sigma_2+\sigma_3)}\varepsilon_1 \tag{20}$$

$$\varepsilon_3 = \frac{\sigma_3-\mu(\sigma_1+\sigma_2)}{\sigma_1-\mu(\sigma_2+\sigma_3)}\varepsilon_1 \tag{21}$$

where σ_2 is the intermediate principal stress and μ is the Poisson's ratio of the soil and is equal to $K_o(1 + K_o)$. K_o is the coefficient of earth pressure at rest. The strain in the vertical direction for each layer is calculated from the following equation:

$$\varepsilon_z = \varepsilon_1\cos^2\theta_1 + \varepsilon_2\cos^2\theta_2 + \varepsilon_3\cos^2\theta_3 \tag{22}$$

in which θ_1, θ_2 and θ_3 are directions of the principal strains with respect to the vertical.

9. The vertical settlement, ΔS, of any layer is computed by multiplying the strain ε_z with the thickness of each layer, δ_z, as follows :

$$\Delta S = \varepsilon_z \cdot \delta_z \tag{23}$$

10. The total settlement, S, along any vertical axis, x, is computed by numerically summing the settlements.

$$S = \sum_{0}^{n} \varepsilon_z \cdot dz \tag{24}$$

11. The total settlements have been computed along various vertical sections, namely, x = $-B/2$, $-4B/10$, $-3B/10$, $-2B/10$, $-B/10$, 0, $B/10$, $2B/10$, $3B/10$, $4B/10$, $B/2$ for the given pressure intensity, eccentricity, angle of inclination and the annular ratio.

The typical settlement pattern obtained by the above procedure for smooth flexible ring footing will be as shown in Figs.7a and 8a respectively for $e/B \leq \left[(1+n^2)/8\right]$ and $e/B > \left[(1+n^2)/8\right]$.

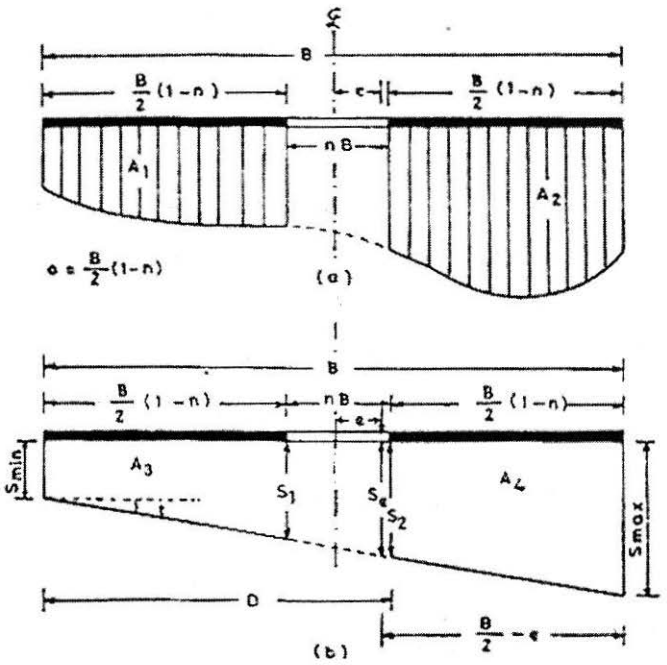

FIGURE 7 : Settlement Diagrams Under Ring Footing (when $e/B \leq \left[(1+n^2)/8\right]$

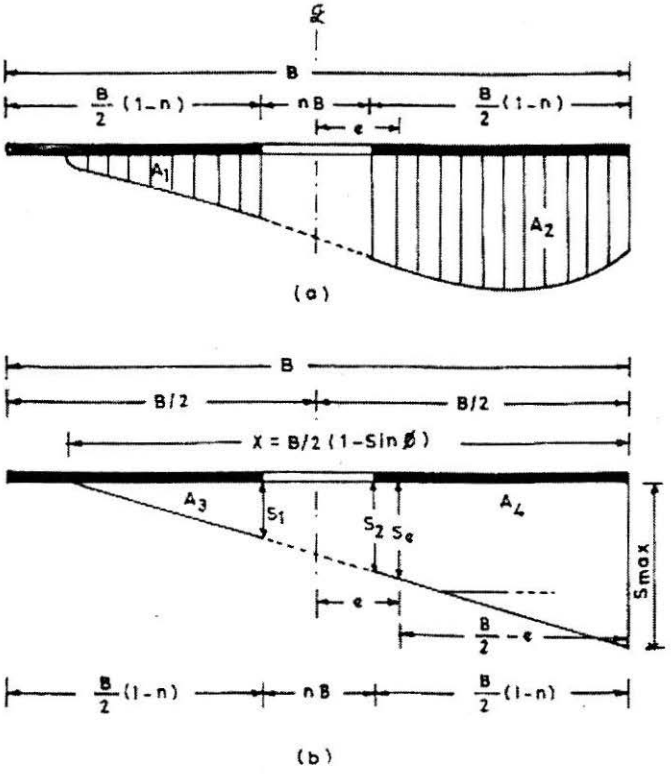

FIGURE 8 : Settlement Diagrams Under Ring Footing (when $e/B > \left[\left(1+n^2\right)/8\right]$

Procedure of Obtaining Settlement and Tilt of A Rigid Ring Footing

In this section, an empirical but logical method has been suggested to obtain the settlement and tilt of a rigid ring footing from the settlement pattern of a flexible ring footing as obtained in Figs.7a and 8a. A rigid ring footing will settle as shown in Fig.7b and 8b. For evaluating the settlement pattern of rigid ring footings, following procedure is adopted:

Case 1 when $e/B \leq \left[\left(1+n^2\right)/8\right]$

The values of S_{max} and S_{min} of a rigid ring footing (Figs.7b) are obtained by equating:

i) The area of settlement diagram of Fig.(7a) to the area of settlement diagram of Fig.(7b) and

ii) The distance of the centre of settlement diagram of Fig.(7a) from the left edge of the footing, i.e. point 'A', to the distance of centre of settlement diagram of Fig.(7b) from the left edge of footing, point 'A'.

i.e. $$A_1 + A_2 = A_3 + A_4 \tag{25}$$

or $$A_s = \left(\frac{a}{2}\right)\left[\left(S_{max} + S_2\right) + \left(S_1 + S_{min}\right)\right] \tag{26}$$

and

$$C_g = \frac{\left[A_3\left\{\frac{(2S_1 + S_{min})a}{(S_1 + S_{min})3}\right\} + A_4\left\{\frac{(2S_{max} + S_2)a}{(S_{max} + S_2)3}\right\} + D\right]}{(A_3 + A_4)} \tag{27}$$

Solving Eqns.(26) and (27), therefore,

$$S_{min} = A_s \frac{\left[B(4+n)(1+n) - 6C_g\right]}{\left[B^2(1-n)\left(1+n+n^2\right)\right]} \tag{28}$$

and

$$S_{max} = A_s \frac{\left[6C_g - B(1-n)(2+n)\right]}{\left[B^2(1-n)\left(1+n+n^2\right)\right]} \tag{29}$$

where

A_s = Area of settlement diagram Fig.(5a) = $A_1 + A_2$

a = $B/2(1-n)$

S_{min} = Minimum settlement of footing

S_{max} = Maximum settlement of footing

B = Width (= external diameter) of footing

C_g = Centre of gravity of the settlement diagram of Fig.(7a) from point 'A'

n = Annular ratio = (Internal Dia./External Dia.)

D = $B/2(1+n)$

S_1 and S_2 are as defined in Fig.7b

It may be noted that the settlement pattern (Fig.7a) is obtained by the

procedure described in this paper. Therefore the values of A_s and C_g can be conveniently determined. Knowing these values, S_{max} and S_{min} may be obtained using Eqns.28 and 29.

Hence, knowing the values of S_{max} and S_{min}, the tilt (t) of the rigid footing (Fig.7b) may be computed using the following equation:

$$t = \frac{(S_{max} - S_{min})}{B} \tag{30}$$

Case 2 when $e/B > \left[\left(1+n^2\right)/8\right]$

In this case the area of settlement diagram of Fig.(8a) is equated to the area of settlement diagram of Fig.(8b). It gives

$$S_{max} = A_s \frac{2X}{X(X-2Bn)+B^2 n} \tag{31}$$

where X is defined in Eqn.(8). Values of X/R have been given earlier in Table 1 in terms of e/B and n.

Knowing the value of S_{max}, the tilt (t) for the rigid ring footing is given by :

$$t = \frac{S_{max}}{X} \tag{32}$$

Firstly settlement pattern for a flexible ring given set of e/B , α, n and B are computed for different applied load intensities by repeating Step 1 to Step 11. Then using the above procedure, settlement (S_{max}) and tilt (t) are obtained for the rigid ring footing of the same dimensions as of flexible footing. Consequently, the pressure versus maximum settlement (S_{max}) and pressure versus tilt (t) curves can then be obtained for the rigid ring footing subjected to eccentric-inclined load.

Similarly pressure-maximum settlement (S_m), and pressure-tilt (t) curves for other sets of e/B , α, n and B are obtained.

The details of the derivations of the equations used are presented by (Al-Smadi, 1998).

Model Tests

A total of fourteen tests were performed on model ring footings of size (external diameter, B) equal to 200 mm resting on Amanat Garh Sand (D_{10} = 0.15, C_u = 2.0, C_c = 1.39). The sand was placed at a relative density of 70%.

The parameters 'a' and 'b' of the hyperbola were obtained by conducting triaxial compression tests at different confining pressures on sand (D_R = 70%) as follows:

$$1/a = 3800(\sigma_3)^{0.58} \tag{33}$$

$$1/b = 90+3.35\sigma_3 \tag{34}$$

where σ_3 is the confining pressure in kPa.

The details of tests performed are given in Table 2.

Model tests were performed in a tank of size 1250 mm × 1250 mm × 1000 mm high. The load on the footing was applied through a calibrated screw jack in increments. For each increment of load, records were taken for the settlement and tilt of the footing through proper instrumentation. Hence for each test, pressure (load/footing area) versus settlement and pressure

TABLE 2 : Details of Test Performed

Test No.	Annular Ratio (n)	Load Inclination α (Deg.)	e/B Ratio
1	0.0	0	0.0
2	0.0	0	0.1
3	0.0	0	0.2
4	0.0	10	0.0
5	0.0	10	0.1
6	0.0	10	0.2
7	0.0	20	0.0
8	0.0	20	0.1
9	0.0	20	0.2
10	0.4	0	0.0
11	0.4	0	0.3
12	0.4	10	0.3
13	0.4	20	0.3
14	0.6	0	0.0

versus tilt curves were obtained. The details of the procedure are given elsewhere (Al-Smadi, 1998).

Results and Discussion

As mentioned in the text, the main analysis has been developed for smooth flexible ring footing, and then a procedure is given for obtaining the maximum settlement and tilt of smooth rigid footing of the same dimension. Prakash et al. (1984) demonstrated that the effect of roughness on pressure-settlement characteristics of a footing is very small (less than 7.0%), Keeping this in view this analysis is developed for smooth ring footings. In author's opinion, the results may be used for rough footings without losing accuracy.

Validation of the proposed methodology of predicting pressure-settlement and pressure-tilt curves of ring subjected to eccentric-inclined loads have been made in all the fourteen cases mentioned in Table 2. Some typical plots of predicted and observed pressure-settlement and pressure-tilt curves are given in Figs.9 and 10. It is evident from these figures that the predicted values of settlement and tilt tally reasonably well up to approximately two-third of the ultimate bearing pressure. Beyond it, the predicted values of the settlement and tilt are higher than the observed ones. As usually in design, the settlements and tilts are obtained for the working pressure intensity $\left[\approx \text{ultimate earing capacity}/(2.0 \text{ to } 3.0)\right]$, this approach may be used for their estimation with confidence.

A parametric study was also made to study the effect of α, e/B ratio, n and B on the settlement and tilt of the footing. Typical pressure-settlement and pressure-tilt curves are shown in Figs.11 and 12. It was found that for the same pressure intensity both settlement and tilt decreases with the increase in n and B, but increases with the increase in α and e/B ratio.

Conclusions

1. An analytical procedure has been proposed to predict the pressure-vertical settlement and pressure-tilt characteristics of ring footings subjected to eccentric-inclined load resting on cohesionless soils, using the non-linear constitutive laws of such soils. This approach, however, requires predetermination of the ultimate bearing capacity. An equation has been suggested to obtain the same.

2. For the same pressure intensity both settlement and tilt decreases with the increase in n and B, but increases with the increase in α and e/B ratio.

3. Predicted and model test results tally well upto two-third of ultimate bearing pressure.

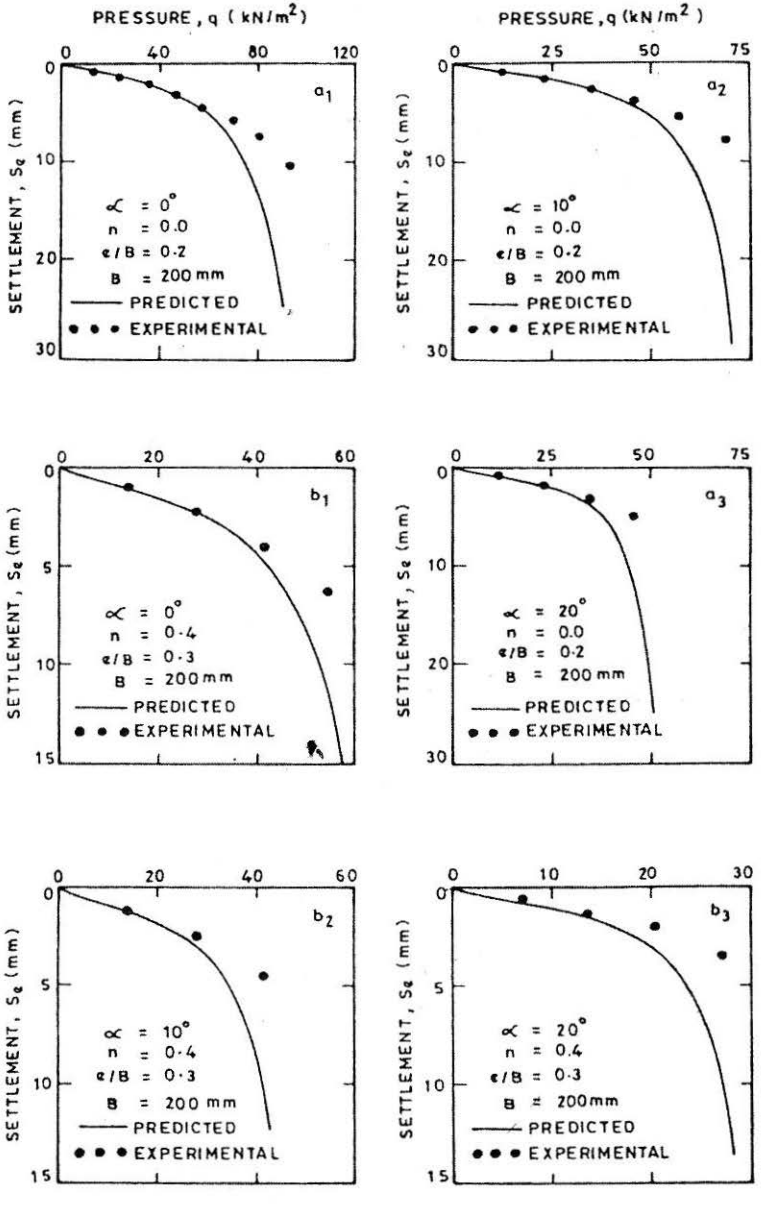

FIGURE 9 : Comparison of Predicted and Experimental Pressure Vs. Vertical Settlement (S_e) Curves for Ring Footing (n = 0.0, 0.4) 0n Unreinforced Amanatgarh Sand (R_D = 70%)

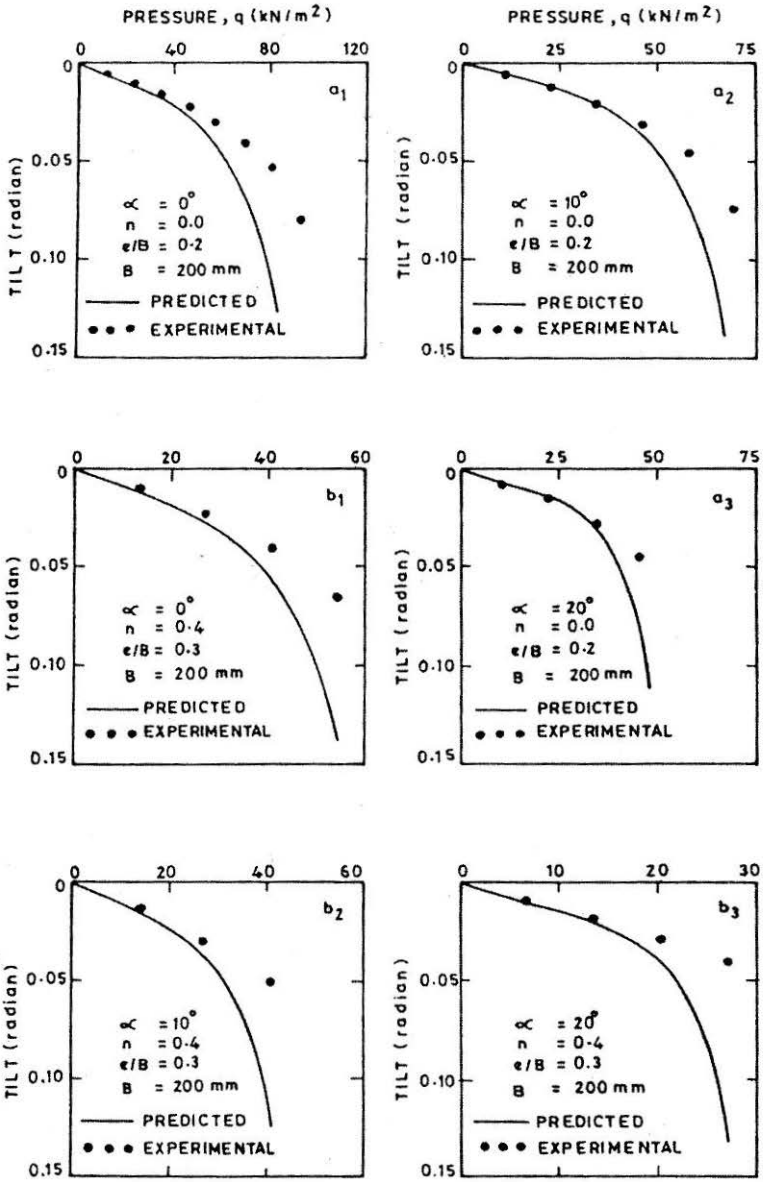

FIGURE 10 : Comparison of Predicted and Experimental Pressure Vs. Tilt Curves for Ring Footings (n = 0.0, 0.4) on Unreinforced Amanatgarh Sand (R_D = 70%)

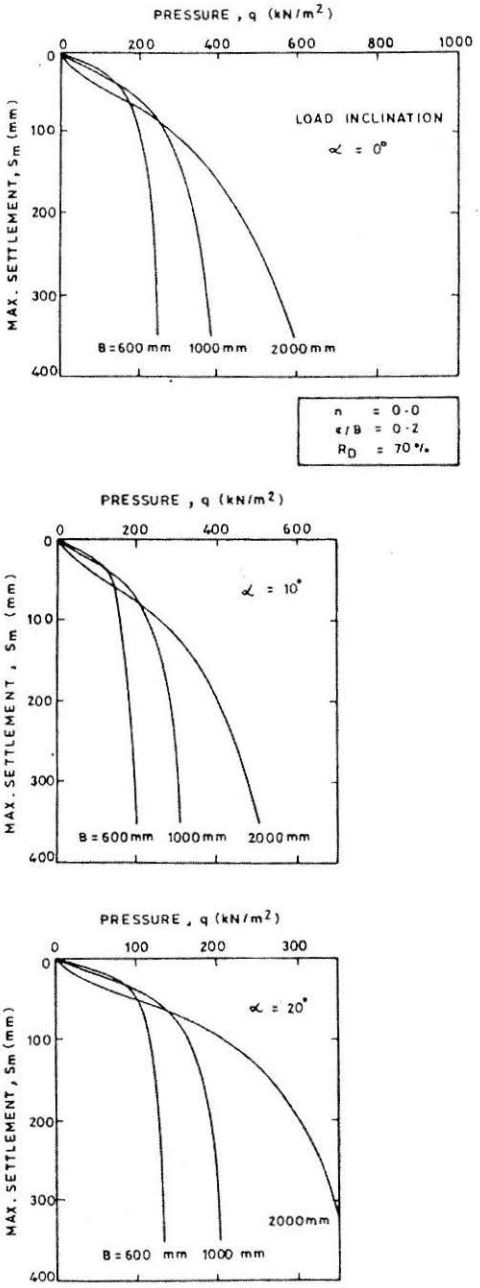

FIGURE 11 : Pressure Vs. Maximum Settlement (S_m) Curves for Ring Footings (n = 0.0), B = 600, 1000, 2000 mm on Unreinforced Amanatgarh Sand for e/B = 0.2

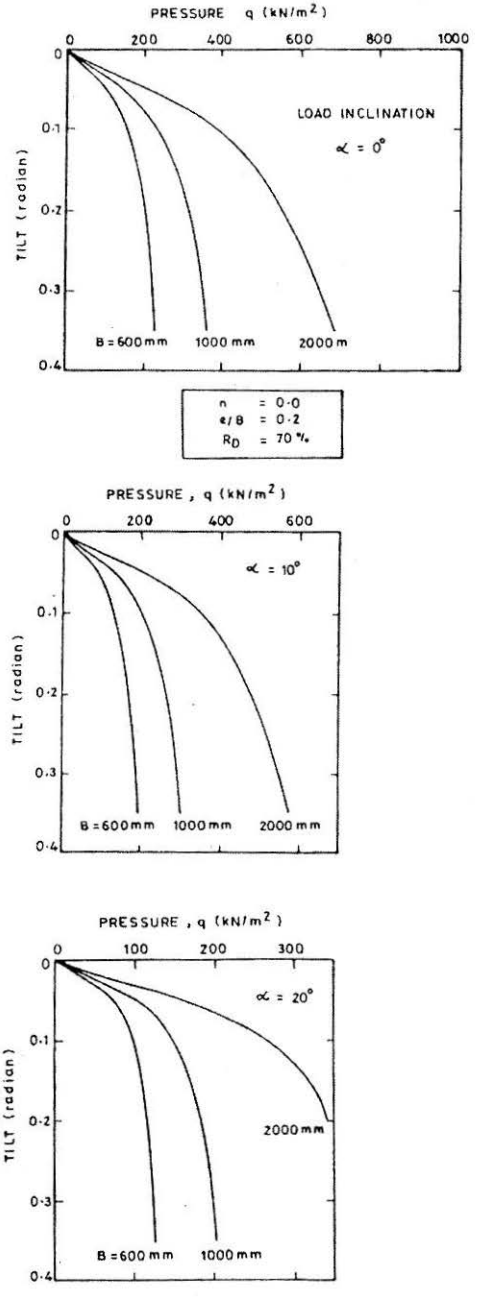

FIGURE 1 : Grain Size DistributionFIGURE 12 : Pressure Vs. Tilt Curves for Ring Footings (n = 0.0), B = 600, 1000, 2000 mm on Unreinforced Amanatgarh Sand for e/B = 0.2

References

AGARWAL, R.K. (1986) : "Behaviour of Shallow Foundations Subjected to Eccentric-Inclined Loads", *Ph.D. Thesis*, University of Roorkee, Roorkee, U.P., India.

AL-SMADI, M.M. (1998) : "Behaviour of Ring Foundations on Reinforced Soil", *Ph.D. Thesis*, University of Roorkee, Roorkee, U.P., India.

BORODACHEVA, F.N. (1968) : "Action of a Vertical Eccentric Force on an Annular Foundation Situated on a Compressible Base", *Soil Mechanics and Foundation Engineering*, No.1, pp.34-37.

BOUSSINESQ, J.V. (1885) : "Applications des Potentiels a L'elude de lequilibre et du Mouvement des Solides Elastique", Paris, Gautheir-Villars, (reported by Jumikis, A.R., 1968, p.76-92).

BOWELS, J.E. (1975) : *Analytical and Computer Methods in Foundation Engineering*, McGraw-Hill Kogakusha Limited, Tokyo, p.196-199.

CERRUTI, V. (1988) : "Sulla Deformazione di un Corpo Elastico Isotropo per Alcne Speciali Condizioni ai Limiti", *R. Academia Nazionale dei Lincei*, Rend. Cont. Ser.4, Vol.4, (Sem.1) : Roma, pp.785-792 (Reported by Jumikis, A.R., 1968, pp.92-95).

CHATURVEDI, A. (1982) : "Behaviour of Eccentrically Loaded Ring Footings on Sand", *M.E. Thesis*, University of Roorkee, Roorkee, U.P., India.

EGOROV, K.E. (1965) : "Calculation of Bed for Foundation with Ring Footing", *Proc. of the 6th International Conference on SMFE*, Montreal, Vol.II, pp.41-45.

HAROON, M. and MISRA, S.K. (1980) : "A Study on the Behaviour of Annular Footings on Sand", *Proc. Indian Geotechnical Conference*, IGC-80, Bombay, Vol.1, pp.87-91.

KAKROO, A.K. (1985) : "Bearing Capacity of Rigid Annular Foundations under Vertical Loads", *Ph.D. Thesis*, University of Roorkee, Roorkee, U.P., India.

KONDNER, R.L. (1963) : "Hyperbolic Stress-Strain Response : Cohesive Soils", *Journal of the Soil Mechanics and Foundations Division*, Proc. ASCE, Vol.89, No.SM1, pp.115-143.

KONDNER, R.L. and ZELASKO, J.S. (1963) : "A Hyperbolic Stress-Strain Formulation for Sands", *Proc. 2nd Pan American Conference on SMFE*, Brazil, Vol.1, pp.289-324.

MILOVIC, D.M. (1973) : "Stresses and Displacements Produced by a Ring Foundation", *Proc. of 8th International Conference on Soil Mechanics and Foundation Engineering*, Vol.III, pp.167-171.

POULOS, H.G. and DAVIS, E.H. (1974) : *Elastic Solutions for Soil and Rock Mechanics*, John Wiley and Sons, Inc., New York.

PRAKASH, S., SARAN, S. and SHARAN, U.N. (1984) : "Footings and Constitutive Laws", *Journal of the Geotechnical Engineering Division*, ASCE, Vol.110, No.10, pp.1473-1488.

ROARK, R.J. (1954) : *Formulas for Stress and Strain*, New York, McGraw Hill Book Company Inc.

SAHA, M.C. (1978) : "Ultimate Bearing Capacity of Ring Footings on Sand", *M.E. Thesis*, University of Roorkee, Roorkee, U.P., India.

TENG, W.C. (1977) : *Foundation Design*, Prentice Hall of India Private Ltd., New Delhi.

YOUNG, W.C. (1989) : *Roark's Formulas for Stress & Strain*, McGraw-Hill Book Company, New York.